New Computational Fluid Dynamic Procedure to Estimate Friction and Local Losses in Coextruded Drip Laterals

Giuseppe Provenzano, Ph.D.[1]; Pietro Di Dio[2]; and Guillermo Palau Salvador, Ph.D.[3]

Abstract: The design of trickle irrigation systems is crucial to optimize profitability and to warrant high values for the emission uniformity (EU) coefficient. EU depends on variation of the pressure head due to head losses along the lines and elevation changes, as well as the water temperature, and other parameters related to the emitters (manufacturer's coefficient of variation, number of emitters per plants, emitter spacing). Trickle irrigation plants are usually designed using small diameter plastic pipes (polyethylene or polyvinyl chloride). The design problem, therefore, needs to consider head losses along the lines as well as emitter discharge variations due to the manufacturer's variability. Variations in the hydraulic head are a consequence of both friction losses along the pipe and local losses due to the emitters' connections, whose importance has been recently emphasized. Since each local loss depends on the emitter type (in-line or on-line) as well as on its shape and dimensions, the morphological variability of the commercially available emitter requires experimental investigations to determine local losses in drip laterals. On the other hand, local losses can be estimated by the mean of computational fluid dynamics (CFD) models, allowing analysis of velocity profiles and the turbulence caused by the emitters' connections. FLUENT software can be considered a powerful tool to evaluate friction and local losses in drip irrigation laterals, after the necessary validation has been carried out by means of experimental data. The main objective of this study was to assess a CFD technique to evaluate friction and local losses in laterals with in-line coextruded emitters. The model was initially used to choose the turbulence model allowing the most accurate estimation of friction losses in small diameter polyethylene pipes, characterized by low Reynolds number. Second, the possibility of using CFD to predict local losses in drip irrigation laterals with a commercially available coextruded emitter was investigated. Simulated local losses were obtained as difference of the total and friction losses along a trunk of pipe, where one single emitter was installed, not considering the emitter outflow. The proposed procedure allows to evaluate local losses for other different emitter models, avoiding tedious and time-consuming experiments.

DOI: 10.1061/(ASCE)0733-9437(2007)133:6(520)

CE Database subject headings: Irrigation; Head loss; Computational fluid dynamics technique; Turbulence; Water management.

Introduction

Water management, aimed to improve irrigation efficiency, is crucial in regions with problems due to water shortage and conflicting water requirements. Microirrigation systems allow one to increase water use efficiency by delivering water directly to the root zones of crops and trees. Emitters and microsprinklers can be classified by their position, as on-line or in-line emitters, or according to the values assumed by the exponent x of the relationship expressing the flow discharge, q [L^3T^{-1}], as a function of the pressure head, h [L]

$$q = kh^x \tag{1}$$

where k [L^3T^{-1}]=coefficient depending on the emitter morphology and behavior. According to the x exponent, emitters can be classified as laminar for $x=1$, turbulent when x ranges between 0.4 and 0.8, and self-compensating when x is close to 0.

The design of microirrigation systems is crucial to increase water use efficiency and to warrant high values for the emission uniformity (EU) coefficient, affected by the variation of pressure head, water temperature, manufacturer's variation, grouping of emitters, clogging, variability in soil hydraulic characteristic, and emitter spacing (Wu 1997).

Each emitter model is characterized by a manufacturer's coefficient of variation (CV). Once the number of emitters per plant and the emitter spacing according to the irrigated crop has been established, it is necessary to limit the variation of the pressure head along the lateral to obtain a certain EU value. Superimposing a range of variability for the pressure heads, and consequently, on the emitter flow rate, is usually considered a valid design criterion for drip laterals (Nakayama and Bucks 1986).

The design procedure needs to consider the variation of the hydraulic head due to pipe elevation changes and head losses along the lines as well as emitter discharge variations for a given operating pressure related to the manufacturing variability, clog-

[1]Associate Professor, I.T.A.F. Dept., Sezione Idraulica, Univ. degli Studi di Palermo, Viale delle Scienze 12, Palermo, Italy 90128. E-mail: gproven@unipa.it

[2]Ph.D. Student, I.T.A.F. Dept., Sezione Idraulica, Univ. degli Studi di Palermo, Viale delle Scienze 12, Palermo, Italy 90128. E-mail: pietrodidi@inwind.it

[3]Associate Professor, Rural Engineering Dept., Polytechnic Univ. of Valencia, Camino de vera sin, 46022, Valencia, Spain. E-mail: guipasal@agf.upv.es

Note. Discussion open until May 1, 2008. Separate discussions must be submitted for individual papers. To extend the closing date by one month, a written request must be filed with the ASCE Managing Editor. The manuscript for this paper was submitted for review and possible publication on February 1, 2006; approved on January 30, 2007. This paper is part of the ***Journal of Irrigation and Drainage Engineering***, Vol. 133, No. 6, December 1, 2007. ©ASCE, ISSN 0733-9437/2007/6-520–527/$25.00.

ging, and water temperature. The head losses within the lateral are essentially constituted by frictional and local losses. The former can be calculated by using the Darcy–Weisbach equation

$$h_r = f(R, k/D_i)\frac{v^2}{2gD_i}L \quad (2)$$

in which h_r=frictional losses; f=friction factor depending on the Reynolds number, R, and on the relative pipe roughness; k/D_i; k=absolute pipe roughness; D_i=internal diameter of the pipe; v=mean flow velocity; g=acceleration attributable to gravity; and L=pipe length.

For smooth pipes, the friction factor is only a function of R, and it is often estimated by the Blasius equation (Blasius 1913) or similar equations obtained by other authors (Bagarello et al. 1995; von Bernuth and Wilson 1989), as well as empirical equations like the Hazen–Williams or the Prandtl equations. Some of these relationships, however, characterized by a simple mathematical form, neglect the variability of the friction factor with the flow conditions.

Local losses are due to the emitter connections, introducing additional turbulence into the pipe; although a single emitter produces a generally small local loss, the total amount of local losses, due to the high number of emitters installed along a lateral, can become a significant fraction of total losses, as recognized by many authors (Howell and Barinas 1980; Jeppson 1982; Al Amoud 1995; Bagarello et al. 1997).

Despite the fact that studies with different kinds of emitters have been carried out by different researchers over the last years (Howell and Hiler 1974; Al Amoud 1995), none of them proposed any general procedure to calculate local losses. Other authors, following the experimental approach and under the hypothesis to neglect the influence of the emitter shape on the local losses, obtained empirical equations to predict local losses within a lateral with on-line or in-line coextruded emitters (Bagarello et al. 1997; Provenzano et al. 2005a). Such equations allow one to evaluate the α coefficient, expressing local losses as a fraction of the kinetic head (De Marchi 1954), as a function of the ratio between the emitter and the pipe diameters, whose values in the experiments ranged between 1.0 and 1.2.

On the other hand, computational fluid dynamics (CFD) techniques have become an important tool to predict flow behavior and to design hydraulic devices in many industrial and engineering processes. CFD codes solve the main equations of fluid dynamics (mass conservation, momentum, and energy equations) in order to obtain average values of pressure and velocity in the control volumes defined by a grid. CFD has been very helpful in studies of valves, pumps, and cavitation, and can be useful, after the necessary validation, to improve the geometry of hydraulic devices (Davis and Stewart 2002; Palau Salvador et al. 2004a).

Recently, Palau Salvador et al. (2004b) proposed a CFD approach to evaluate the local losses due to on-line emitter connections. In particular, local losses produced by two different models were simulated on the basis of the turbulence analysis around the emitter connection. The Reynolds stress model was used in order to obtain a simulation of the local losses produced by the protrusion area of the emitter. The model represented accurately the log-law velocity distribution near the wall (Schilichting 1980) as well as the drop pressure obtained from the experimental tests.

Due to the enormous amount of commercially available on-line and in-line emitters, characterized by different shape and geometry, the use of CFD can allow one to evaluate local losses caused by the emitters' connections, avoiding tedious and time-consuming experiments. Nevertheless, it is relevant to highlight the importance of the experimental validation and theoretical discussion of the numerical results for their interpretation and analysis.

Hence, the paper proposes a CFD procedure to evaluate pressure losses in laterals with in-line coextruded emitters. Initially, a sensitivity analysis was carried out in a small diameter polyethylene pipe in order to establish which turbulence model allows the best evaluation of the flow resistance law parameters, and consequently, the accurate prediction of friction losses. Both the influence of the mesh and the boundary layer were initially investigated in a trunk of pipe without an emitter, with the aim to find the best spatial discretization for the simulations. Finally, the possibility of using CFD to predict local losses due to a commercially available coextruded emitter, welded on a polyethylene pipe, has been investigated. Local losses, calculated as the difference of the total and the friction losses along the pipe obtained by means of simulations and for different R, where then compared with those experimentally obtained by Provenzano and Pumo (2004), in order to evaluate the accuracy of the proposed approach.

Turbulence Models

The commercially available CFD code, FLUENT Version 6.1 (Fluent Europe 2001a) is based on the finite-volume method (Veersteg and Malalasekera 1995). A Newtonian and incompressible fluid are assumed in steady-state flow. The governing equations, neglecting the energy equations, were solved by using the SIMPLE algorithm (Patankar 1980). Conservation of mass and momentum equations are as follows:

$$\frac{\partial u}{\partial x} + \frac{\partial v}{\partial y} + \frac{\partial w}{\partial z} = 0 \quad (3)$$

$$\rho\left(\frac{\partial \mathbf{V}}{\partial t} + (\mathbf{V}\cdot\nabla)\mathbf{V}\right) = -\rho g z - \nabla\mathbf{P} + \nabla\tau^{*} \quad (4)$$

where u, v, and w $[LT^{-1}]$=component of velocity along the directions x, y, and z, respectively, $\mathbf{V}$ $[LT^{-1}]$=mean velocity vector; ρ $[FT^2L^{-4}]$=fluid density, ∇=vector operator ($\nabla=\partial/\partial x + \partial/\partial y + \partial/\partial z$); g $[LT^{-2}]$=gravity acceleration; z[L]=height; $\mathbf{P}[FL^{-2}]$=static pressure; and $\nabla\tau^{*}[FL^{-2}]$=divergence of the stress tensor. The number of unknown variables turns out to be 13 (velocity components, pressure, and stress field), making Eqs. (3) and (4) difficult to be solved. However, calculations are simplified introducing the Navier–Stokes equations. The turbulence model chosen to solve Eqs. (3) and (4) was a modified $k-\varepsilon$ model. It is characterized by two transport equations, one for the turbulent kinetic energy, k, and the other for the rate of the dissipation of turbulent kinetic energy, ε, respectively. The modification of the model refines the prediction of the flow behavior near the wall for cases characterized by low-Reynolds numbers. The FLUENT CFD code allows one to consider six models modifying the standard $\kappa-\varepsilon$ model. In particular, the models proposed by Abid (1993), Lam and Bremhorst (1981), Launder and Sharma (1974), Yang and Shih (1993), Abe et al. (1994), and Chang et al. (1995) were used in a preliminary study in order to establish which model better predicts the friction losses in a smooth pipe with R ranging from about 4,000 to 20,000 (Provenzano et al. 2005b). These results showed that the Yang–Shih (YS) model (Yang and Shih 1993) had the best results in terms of magnitude of predicted friction losses and represent the turbulence near the wall. Hence,

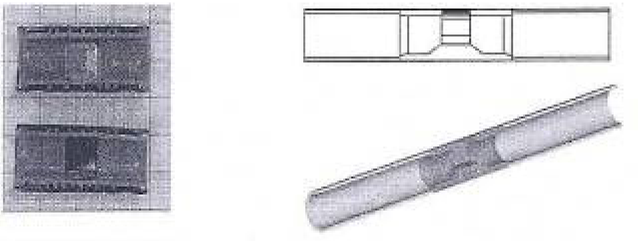

RAINBIRD Gocciatub

'ig. 1. Pictures and geometric scheme of the considered emitter

s low-Reynolds turbulence model was chosen in this paper for imating the local losses produced by an integrated emitter for ferent Reynolds numbers.

ıterials and Methods

ıysical System

;. 1 shows the commercial in-line emitter model, considered in present investigation (RAINBIRD Gocciatub), which results coaxial to the pipe. Table 1 shows the geometry of pipe–itter systems and the range of flow rates and Reynolds num-s considered in the simulations; flow rates were assumed equal those measured during the experiments allowing the measure-nt of local losses (Provenzano and Pumo 2004). The value of emitter diameter, D_g, was assumed to be equal to the corre-nding equivalent coaxial diameter.

The CFD numerical procedure was initially performed by ısidering a 30-cm-long trunk of pipe without emitters in order choose the turbulence model and the parameters defining boundary layer and the mesh. A three-dimensional computa-ıal grid was generated using the package GAMBIT 2.1 (Fluent ope 2001b). The computational domain was meshed using boundary layer having the dimension of the first row, 0.002 mm, a growth factor (ratio between consecutive rows) 1.15 and a number of rows $N=40$, and considering a struc-ed mesh with dimension of 1 mm (Simulation 1, SIM. 1), as strated in Fig. 2. As shown in Fig. 2 the flow direction was ımed along the x axis, whereas the z and y axes defined the ıar pipe section perpendicular to the flow direction.

For each simulation the inlet boundary condition, expressed in ns of velocity profile, was specified. The velocity components well as the k and ε parameters were iteratively obtained; ini-ly, all the considered variables were assumed constant at the tream end of the pipe (I iteration); the velocity profile and the values obtained at the downstream end were then considered e the starting values for the second iteration, and so on with following iteration. Simulations were carried out considering six turbulence models modifying the standard κ–ε.

To verify the influence of the boundary layer, other simu-ons were conducted by considering the YS model with $a=0.02$ mm, $g_f=1.15$, and $N=24$ and mesh equal to 1 mm (SIM. 2) as well as with $a=0.2$ mm, $g_f=1.10$, and $N=10$ and mesh equal to 0.7 mm (SIM. 3). Mesh sensitivity was also initially tested with smaller cell sizes, but no influence on the final results was found. Simulations were successively performed in a trunk of pipe, still having a length of 30 cm, in which one coextruded emitter was introduced 7 cm downstream the pipe inlet.

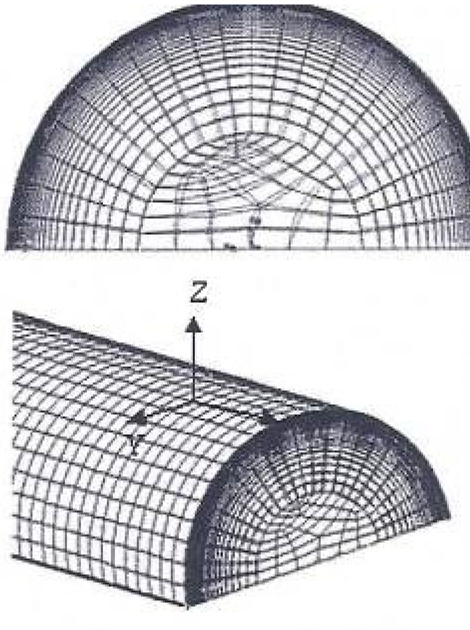

Fig. 2. View of the boundary layer and the grid used for the simulations (pipe without emitter)

Three different flow domains were defined. In the first (7 cm) and in the last trunk of pipe (23 cm), a structured mesh, identical to that previously used for the simple pipe was defined, while in the middle domain and for the entire emitter's length, an unstruc-tured grid was built. In the latter simulations the velocity profile at the pipe inlet was assumed equal to the outlet profile obtained in the third iteration for the same R and considering the pipe without emitter. The cell size chosen was 1.0 mm in all the ex-amined cases. In all the simulations a symmetry boundary plane mirror, containing the pipe axis, was defined in the middle of the pipe, in order to decrease the number of nodes and the calculation time.

Results and Discussion

After three simulations, the velocity profile was identical in the entire considered domain. Therefore, the slope of the energy gra-dient line along the longitudinal axes of the pipe was constant, suggesting that three simulations were sufficient to evaluate pipe friction losses.

ıle 1. Geometry of the Considered Pipe Emitter Systems and Variability Range of Flow Rates ($Q_{min} \div Q_{max}$) and Reynolds Numbers ($R_{min} \div R_{max}$) sidered in the Experiments

tter	D_i (mm)	D_g (mm)	L_g (mm)	D_i/D_g (−)	$Q_{min} \div Q_{max}$ (l/h)	$R_{min} \div R_{max}$ (−)
ciatub	13.76 (0.09)	11.60 (0.21)	35.60 (0.07)	1.186	128.7 ÷ 603.8	3,437 ÷ 15,759

e: D_i=pipe internal diameter; D_g=emitter equivalent internal diameter; and L_g=emitter length. Standard deviation is indicated in parentheses.

Table 2. Simulated and Calculated Friction Losses per Unit Pipe Length Obtained with the AKN (Abe et al. 1994) and the Modified Blasius Equations (Bagarello et al. 1995), Respectively, for Different R Values

v (m/s)	R (–)	AKN [J (Pa/m)]	Bagarello et al. (1995) [J (Pa/m)]	D (%)
0.374	5,913	194.54	181.30	−7.3
0.475	7,592	292.55	274.72	−6.5
0.739	11,677	635.10	597.11	−6.4
1.007	15,569	1,065.98	1031.79	−3.3
1.181	18,673	1,452.78	1,356.10	−7.1
1.363	20,632	1,892.72	1,761.78	−7.4

Note: Differences between simulated and calculated values, expressed as percentage of the calculated ones, are also shown.

Table 2 shows the comparison between friction factor simulated for different Reynolds numbers and D_i=13.76 mm, with the YS model and the corresponding values obtained by using the modified Blasius equation proposed by Bagarello et al. (1995). As it can be seen from Table 2 the simulated friction losses were slightly higher compared to the calculated ones, with differences, in absolute value, never higher than 7.4%.

Furthermore, Table 3 illustrates, for the different R, the friction losses obtained in the three groups of simulations, considering different boundary layers and meshes. The differences between the simulated and the calculated friction losses, expressed as a percentage of the calculated ones, are also indicated. As can be noted in Table 3, for all the considered R values, the differences between the simulated and estimated friction losses obtained assuming a less detailed boundary layer (SIM. 2), even if associated to a finer mesh (SIM. 3), were higher than the corresponding values obtained in simulation 1 (SIM. 1). All the following simulations were, therefore, made considering the boundary layer and the mesh associated with SIM. 1.

Figs. 3(a–c) show the velocity profiles in the middle of the considered trunk of pipe (D_i=13.76 mm), obtained considering the YS turbulence model and R=4,322, 10,972, and 15,758, respectively. As can be observed in Fig. 3, for all the considered R, YS model accurately represents the velocity profile near the wall, as well as the logarithmic velocity distribution law, valid for turbulent flow in smooth pipe. A transition zone from the laminar sublayer to the completely developed turbulent flow can also be observed. Similar results were obtained for the other investigated R values.

The results confirm the accuracy of the YS model to estimate friction losses in small diameter polyethylene pipes with low turbulent R values, because it allows one to take into account the two regions in which the flow can be considered divided,

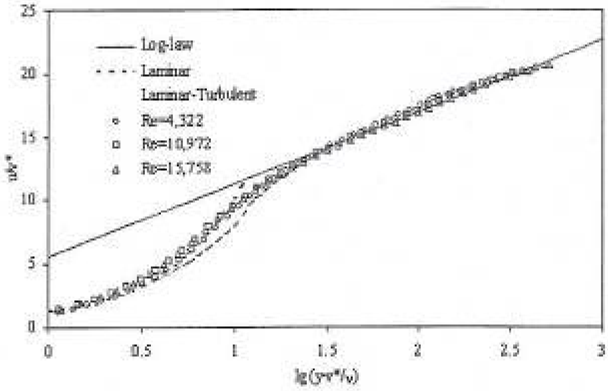

Fig. 3. Velocity profiles in the middle of the considered trunk of pipe without emitter (D_i=13.76 mm) obtained for R=4,322, 10,972, and 15,758

i.e., the thin layer in the vicinity of the pipe (boundary layer), where friction plays an essential part and the remaining region outside this layer, where friction can be neglected. The results show also the adequacy of the boundary layer and the mesh parameters representing the computational domain.

Figs. 4(b–d) show, for the six different pipe sections shown in Fig. 4(a), the dimensionless velocity distributions u/U (u=punctual velocity; U=flow velocity averaged in the pipe section), obtained along the directions z, y^+, and y^-, respectively. Since the emitter is uncoaxial and considering that there is no symmetry along the y axes, it was necessary to consider separately both y^+ and y^- velocity distributions. As can be seen in Fig. 4(b), the effect on the velocity profile attributable to the streamline contraction in the middle of the emitter (Section P2) can be recognized; the velocity profile is flatter than the previous sections due to the highest R value inside the emitter, corresponding to the highest turbulence. On the other hand, along the y^+ axis differences were observed between the velocity profiles at P1 compared to the inlet pipe section. In the middle of the emitter (Section P2) a different velocity profile was observed between y^+ and y^- directions. In the former the velocity profile decreases and increases again due to a vortex causing the flow recirculations close to the pipe wall. In the latter a flatter velocity profile can be noticed, similar to that observed along the z direction. By comparing the velocity profiles at the P3 section along both y^+ and y^- axes it is easily verifiable that the jet is displaced below the pipe axis, as a consequence of the absence of symmetry along the emitter.

Table 3. Simulated Friction Losses Obtained in the Three Simulations and Percentage Differences Calculated Adapting the Modified Blasius Equation, Suggested by (Bagarello et al. 1995)

		SIM. 1		SIM. 2		SIM. 3	
V (m/s)	R (–)	J (Pa/m)	D (%)	J (Pa/m)	D (%)	J (Pa/m)	D (%)
0.374	5,913	194.54	−7.3	207.48	−14.4	228.0	−25.8
0.475	7,592	292.55	−6.5	312.27	−13.7	346.0	−25.9
0.739	11,677	635.10	−6.4	681.26	−14.1	707.3	−18.5
1.007	15,569	1,065.98	−3.3	1,187.76	−15.1	1,085.6	−5.2
1.181	18,673	1,452.78	−7.1	1,571.85	−15.9	1,320.4	2.6
1.363	20,632	1,892.72	−7.4	2,050.78	−16.4	1,667.5	5.4

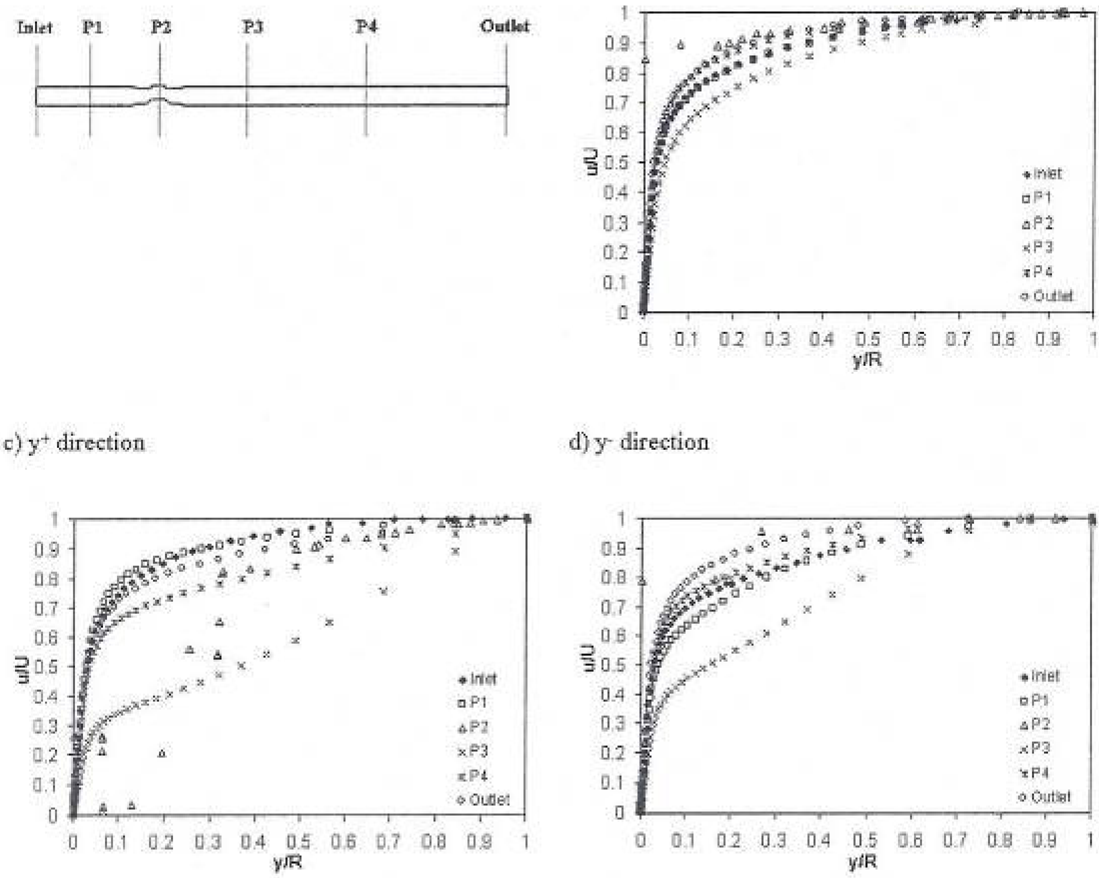

Fig. 4. (a)–(d): Dimensionless velocity distribution obtained in the six different pipe sections showed on the upper-left scheme

Fig. 5 shows the logarithmic velocity distribution law obtained along the z direction in the different pipe sections considered in Figs. 4(a), obtained for R=15,758. Fig. 5 confirms that the most disturbed velocity profiles can be recognized in the middle and just downstream from the emitter.

Figs. 6(a–c) show the simulated total head H, along the considered trunk of pipe, obtained for three different Reynolds numbers and by using the YS model; the secondary axis shows the slope of the energy gradient line under the same flow conditions. As it can be seen in Figs. 6(a–c), the slope of the energy gradient line is constant before the emitter, strongly increases along the emitter, and tends to assume the initial value downstream from the emitter (fully developed flow). A slowly increasing slope of the energy gradient line can be observed immediately downstream from the emitter, resulting from higher R values. In particular, the jet downstream the emitter is surrounded by a stationary solid surface separating a thin layer of fluid.

Obviously for the considered emitters, the higher the R is the larger the head loss caused by the emitter connections. Moreover, as it can be observed in Fig. 6, the turbulence produced by the emitter can be considered extinguished along the considered length.

Fig. 7 shows the cumulative differences, Λ, between the simulated total losses along the trunk of the pipe with the emitter and the corresponding values obtained considering the pipe without the emitter, for R=4,322 and 15,75 respectively.

Fig. 7 shows that the local losses due to the streamlines cc traction are smaller than those corresponding to the conseque enlargement. In addition along the emitter's length a higher he loss due the smaller diameter of the emitter compared to the pi one is confirmed by the higher slope of the $\Lambda(x)$ functions.

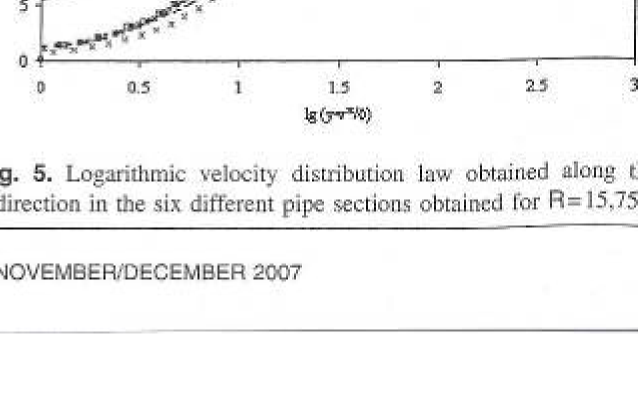

Fig. 5. Logarithmic velocity distribution law obtained along t z-direction in the six different pipe sections obtained for R=15,75

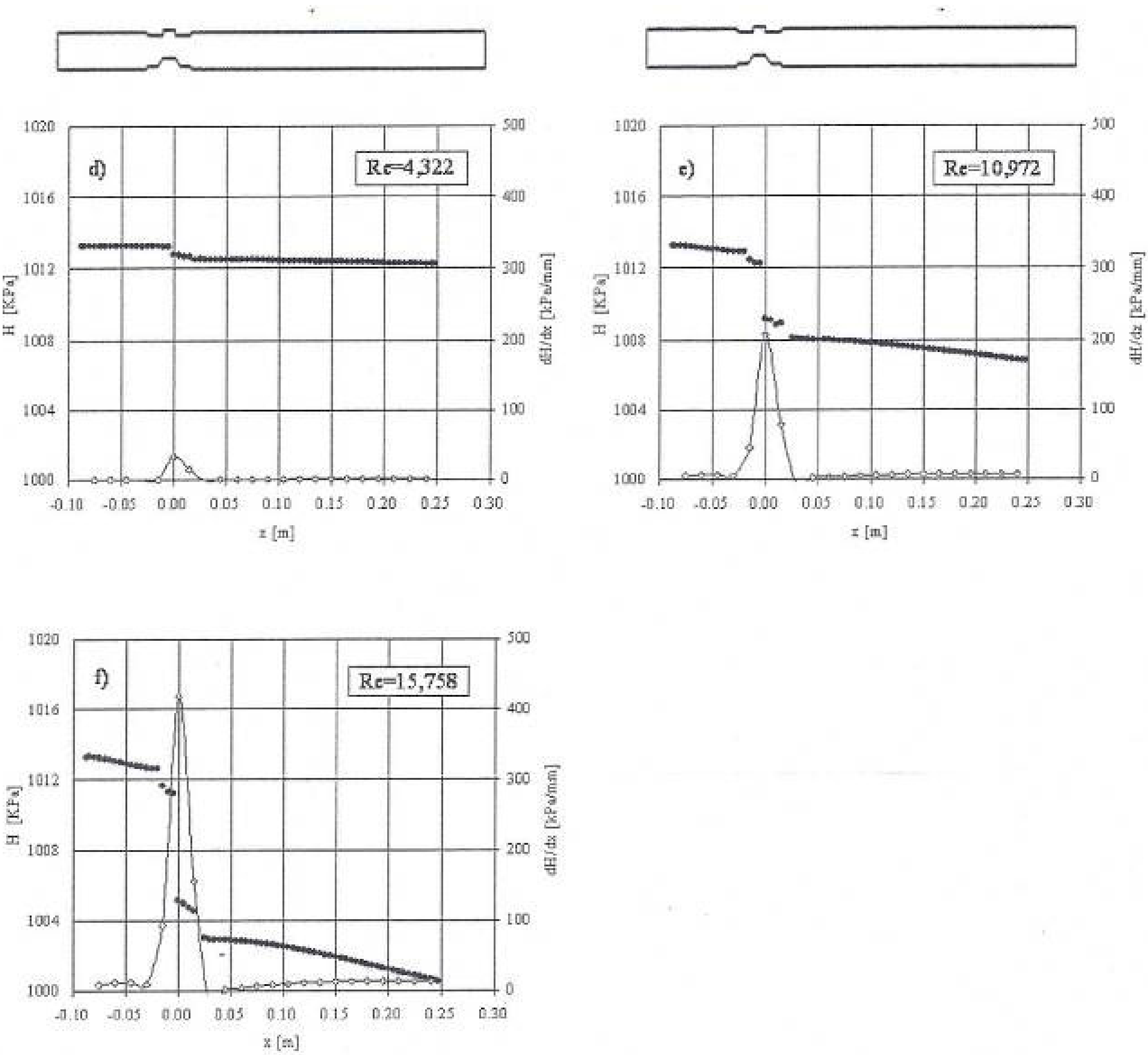

Fig. 6. (a)–(c): Simulated total pressure head, H, along the considered trunk of pipe for three different R values. Variation of total pressure head, dH/dx, are shown in the secondary axis.

Fig. 8 illustrates the velocity contours obtained for R = 15,758. As can be observed the velocity contours are evenly distributed upstream of the emitter and a vortex producing a redirected flow can be noticed in the close up. Fig. 8 also shows that the jet axis results below the pipe one, as illustrated and discussed in Figs. 4(b and d).

For each R, the value of the α coefficient was then calculated dividing for the kinetic head of the flow, the difference between the head losses simulated in the pipe with the emitter and the corresponding value obtained considering the pipe without the emitter. Each α value so calculated represents the local losses due to the introduction of the emitter into the pipe and takes into account both the head losses caused by the contraction and enlargement of the streamlines as well as the major head loss due to the emitter diameter, which is smaller than the pipe diameter. Table 4 shows the simulated and the measured α values calculated by using the experimental data of Provenzano and Pumo (2004); the differences D between simulated and measured α values, expressed as percentage of the measured ones, are also shown in Table 4. Despite a slight overestimation of the simulated alpha values in Table 4, these results indicate that the CFD procedure can be used to evaluate local losses due to the emitter connections, avoiding the need for repeated expensive and time-consuming experiments.

Conclusions

The investigation assessed the feasibility of a CFD technique to evaluate friction and local losses in laterals where in-line coextruded emitters are installed. The FLUENT model was initially

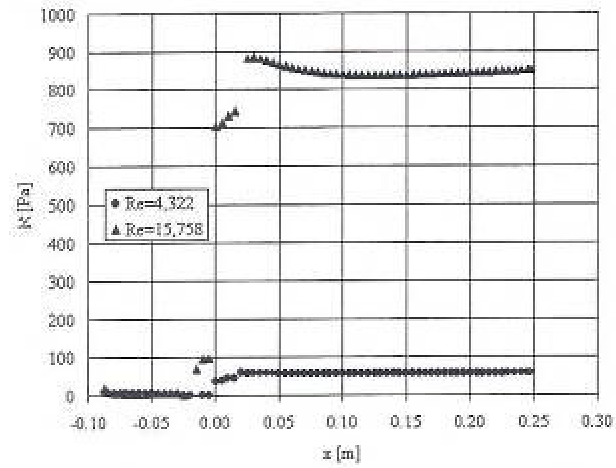

Fig. 7. Cumulative differences Λ between the total losses obtained considering the trunk of pipe with and without the emitter and for two different R values

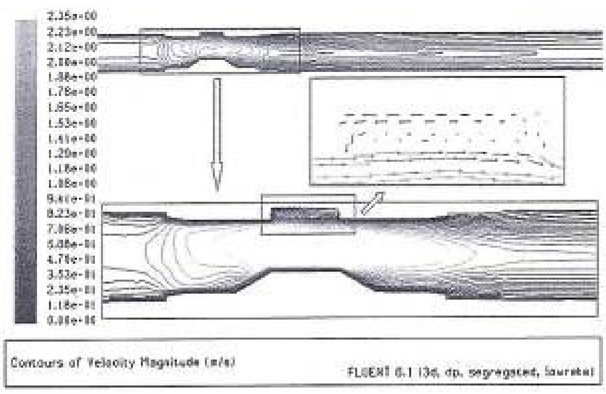

Fig. 8. Velocity contours in the pipe–emitter system obtained for R=15,758

Table 4. Simulated and Measured α Values Obtained for Different R

R	α Simulated	α Measured	D (%)
4,322	1.62	1.50 (0.08)	8.0
5,528	1.64	1.42 (0.06)	15.5
8,441	1.50	1.36 (0.03)	10.3
10,972	1.45	1.34 (0.01)	8.2
14,122	1.42	1.34 (0.01)	6.0
15,758	1.41	1.33 (0.08)	6.0

Note: Differences between simulated and measured values, expressed as percentage of the measured ones, are also shown. Standard deviations of the measured values are showed in parenthesis.

used in order to analyze the turbulent regime in a small diameter polyethylene pipe and to establish the model providing the best prediction of the friction losses. A very detailed structured mesh and boundary layer was assumed in order to get the best results in terms of simulated friction losses. Secondly the CFD was used to predict the coefficient α of the flow kinetic head permitting the evaluation of the local losses.

The simulations carried out showed that the CFD technique can simulate with reasonable accuracy head losses in polyethylene pipes in the range of Reynolds numbers, typical of the low-turbulence regime. Moreover, the comparison between simulated and measured α coefficients indicates the possibility of estimating the local losses due to the emitter connections using the CFD technique and avoiding expensive and time consuming experiments. Further investigations will be carried out in order to extend the proposed calculation procedure to other emitter models commercially available, characterized by a different connection shape and geometry.

Acknowledgments

This research was supported by Università di Palermo. The writers wish to thank the International Cooperation Office (CORI), to support the cooperation with the Universidad Politécnica de Valencia.

References

Abe, K., Kondoh, T., and Nagano, Y. (1994). "A new turbulence model for predicting fluid flow and heat transfer in separating and reattaching flows. I. Flow field calculations." *Int. J. Heat Mass Transfer*, 37(1), 139–151.

Abid, R. (1993). "Evaluation of two-equation turbulence models for predicting transitional flows." *Int. J. Eng. Sci.*, 31(6), 831–840.

Al Amoud, A. I. (1995). "Significance of energy losses due to emitter connections in trickle irrigation lines." *J. Agric. Eng. Res.*, 60(1), 1–5.

Bagarello, V., Ferro, V., Provenzano, G., and Pumo, D. (1995). "Experimental study on flow resistance law for small diameter plastic pipes." *J. Irrig. Drain. Eng.*, 121(5), 313–316.

Bagarello, V., Ferro, V., Provenzano, G., and Pumo, D. (1997). "Evaluating pressure losses in drip irrigation lines." *J. Irrig. Drain. Eng.*, 123(1), 1–7.

Blasius, H. (1913). "Das aehnlichkeitsgesetz bei reibungsvorgangen in flussigkeiten." *Forshhungsarbeiten auf dem gebiete des ingenieurwesen*, Germany, 131(1) (in German).

Chang, K. C., Hsieh, W. D., and Chen, C. S. (1995). "A modified low-Reynolds-number turbulence model applicable to recirculating flow in pipe expansion." *ASME J. Fluids Eng.*, 117, 417–423.

Davis, J. A., and Stewart, M. (2002). "Predicting globe control valve performance. Part I: CFD modeling." *ASME J. Fluids Eng.*, 124, 772–777.

De Marchi, G. (1954). *Idraulica. Basi Scientifiche e applicazioni tecniche*, U. Hoepli, ed., Milano, Italy (in Italian).

Fluent Europe. (2001a). *FLUENT users' manual. Version 6.1*, Fluent Europe Ltd., Sheffield, U.K.

Fluent Europe. (2001b). *GAMBIT users' manual. Version 2.1*, Fluent Europe Ltd., Sheffield, U.K.

Howell, T. A., and Barinas, F. A. (1980). "Pressure losses across trickle irrigation fittings and emitters." *Trans. ASAE*, 23(4), 928–933.

Howell, T. A., and Hiler, E. A. (1974). "Designing trickle irrigation laterals for uniformity." *J. Irrig. and Drain. Div.*, 100(4), 443–454.

Jeppson, R. W. (1982). *Analysis of flow in pipe networks*, 5th Ed., Ann Arbor Science, Ann Arbor, Mich.

n, C. K. G., and Bremhorst, K. A. (1981). "Modified form of the κ-ε model for predicting wall turbulence." *J. Fluids Eng.*, 103, 456–460.

ınder, B. E., and Sharma, B. I. (1974). "Application of the energy dissipation model of turbulence to the calculation of flow near a spinning disk." *Lett. Heat Mass Transfer*, 1, 131–138.

ĸayama, F. S., and Bucks, D. A. (1986). *Trickle irrigation for crop production*, Elsevier Science, Amsterdam, The Netherlands.

au Salvador, G., Arviza Valverde, J., and Bralts, V. (2004a). "Flow behavior through an in-line emitter labyrinth using CFD techniques." *Proc. ASAE/CSAE Annual Int. Meeting*, Ottawa, Canada.

au Salvador, G., Arviza Valverde, J., Gonzàlez-Altozano, P., Royuela Tomas, A., and Provenzano, G. (2004b). "Evaluating pressure losses in drip irrigation laterals using computational fluid dynamic techniques (CFD)." *Proc., European Ageing Conf.*, Leuven, Belgium.

ankar, S. V. (1980). *Numerical heat transport and fluid flow*, Taylor & Francis, New York.

venzano, G., and Pumo, D. (2004). "Experimental analysis of local pressure losses for microirrigation laterals." *J. Irrig. Drain. Eng.*, 130(4), 318–324.

Provenzano, G., Pumo, D., and Di Dio, P. (2005a). "A simplified procedure to design drip irrigation laterals." *J. Irrig. Drain. Eng.*, 131(6), 525–532.

Provenzano, G., Pumo, D., Di Dio, P., Arviza Valverde, J., and Palau Salvador, G. (2005b). "Assessing a computational fluid dynamics technique (CFD) to evaluate pressure losses in coextruded drip laterals." *Proc., ASAE Int. Meeting*, Tampa.

Schilichting, H. (1980). *Boundary layer theory*, McGraw-Hill, New York.

Veersteg, H. K., and Malalasekera, W. (1995). "An introduction to computational fluid dynamics." *The finite volume method*, Longman, New York.

von Bernuth, R. D., and Wilson, T. (1989). "Friction factor for small diameter plastic pipes." *J. Hydraul. Eng.*, 115(2), 183–192.

Yang, Z., and Shih, T. H. (1993). "New time scale based κ-ε model for near-wall turbulence." *AIAA J.*, 31(7), 1191–1198.

Wu, I. P. (1997). "An assessment of hydraulic design of microirrigation systems." *Agric. Water Manage.*, 32, 275–284.